

図 1 AAV ベクター製造性を確認したバキュロウイルスベクターの組み合わせ

その結果、血清型による影響はそれほど大きくなく、むしろ AAV8 型の方が産生量は増加したが、FIX 遺伝子を搭載することで、AAV2 型及び AAV8 型のいずれにおいてもベクターの産生効率は大きく低下し、AsRed2 遺伝子を搭載した時と比較して 1/5 ~ 1/10 以下となった (図 2)。

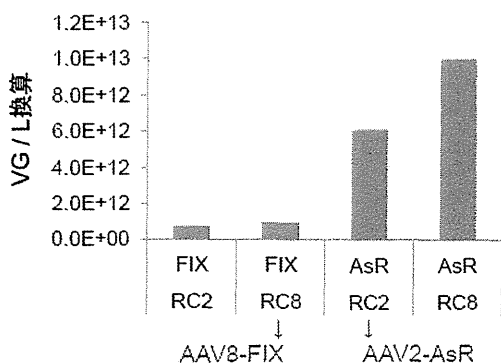


図 2 AAV2 型及び 8 型ベクターにおける AsRed2 及び FIX 遺伝子搭載時のベクター産生性

・ AAV8-FIX ベクター産生性向上の検討：
AAV ベクターを製造するための条件につい

て種々検討を行った。まず、バキュロウイルスベクター感染後の AAV ベクター回収日およびバキュロウイルス感染時の MOI について確認したところ、回収日によってベクター回収率は大きく変動することが確認された。一方 MOI については MOI=10 まで比率を上昇させると AAV ベクター製造効率は低下するが、MOI=1 と 3 ではほとんど差がなかったことから、ある程度の幅においては安定して製造できることが確認された (図 3)。

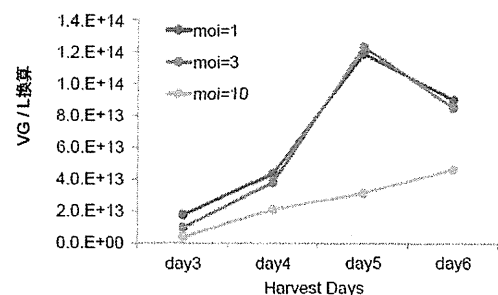


図 3 バキュロウイルス感染時の MOI と AAV ベクター回収日における産生効率

次に市販の昆虫細胞用の培地 3 種類と感染時のセットアップ細胞数について比較した。この際、各条件によって AAV ベクター回収日に影響があることが予想できたため、継続的に回収し産生効率を確認した。その結果、培地種によって産生効率は相当変動し、さらに、各培地において至適セットアップ細胞数も異なることが認められた (図 4)。

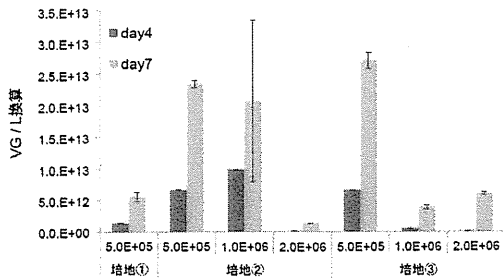


図 4 培養用培地、セットアップ細胞数、回収日による AAV ベクター製造効率の比較

我々が構築したバキュロウイルスベクターによる AAV ベクター産生システムにおいては、2 種類のバキュロウイルスベクターを Sf9 細胞に感染させる。この際、それぞれのベクター比率が AAV ベクター産生効率に影響するかどうかを確認した。しかしながら、どちらか一方のバキュロウイルスベクターの比率を増加させても AAV ベクターの製造量は増加しなかった (図 5)。

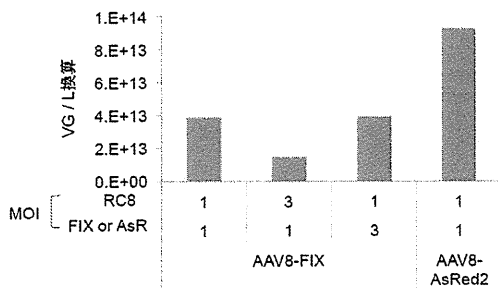
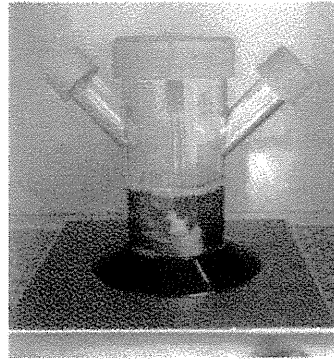


図 5 感染させるバキュロウイルスベクターの比率を変動させた時の AAV ベクター産生効率

このことより各バキュロウイルスベクターはそれぞれ MOI=1 で感染させることで十分であることが確認できた。

・ Sf9MCB 製造条件の検討：これまでに検討を実施してきた三角フラスコによる培養法に近い条件で培養可能であるスピナーフラスコと AAV ベクター実製造時に使用する予定である Wave Bioreactor により Sf9 昆虫細胞の増殖性を検討した (図 6)。

○スピナーフラスコ



○Wave培養システム

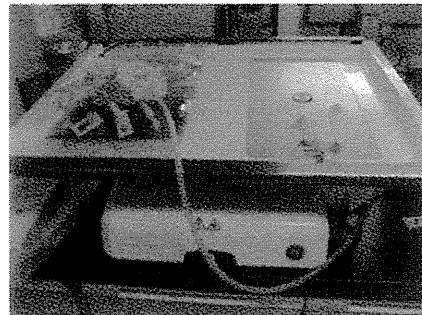


図 6 昆虫細胞大量培養に使用されるスピナーフラスコと Wave 培養システム

スピナーフラスコを用いた場合に Sf9 細胞は順調に増殖が認められ、短期間で一定量以上の MCB が製造できることが確認できた。一方で、Wave Bioreactor を用いた場合には、当初設定した培養条件では細胞増殖がほとんど認められなかった。培養途中で wave の揺動速度を上昇させることで、細胞増殖が確認できるようになったが、安定した MCB 製造のためには、さらなる条件検討が必要と考えられた (図 7)。

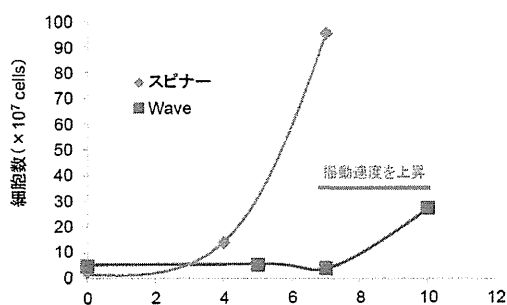


図7 スピナーフラスコと Wave 培養システムにおける Sf9 昆虫細胞の培養

・ AAV8-FIX 実製造大スケール検討：これまでの三角フラスコを用いた小スケール検討の条件を用いて、スピナーフラスコ及び Wave bioreactor での AAV8-FIX ベクター産生効率を確認した。スピナーフラスコにおいては順調な細胞増殖が認められていたが、AAV ベクターはほとんど産生しなかった。一方で、Wave Bioreactor を用いた場合には、細胞増殖の至適条件が見い出せていない段階ではあるものの、三角フラスコでの小スケール検討と同程度の AAV 産生効率を確認できた。すなわち 1L あたり約 $2 \times 10^{13} \text{vg}$ の産生性が得られたことから、150L 培養を行うことで、 $3 \times 10^{15} \text{vg}$ 製造量を確保できる見込みであった (図 8)。

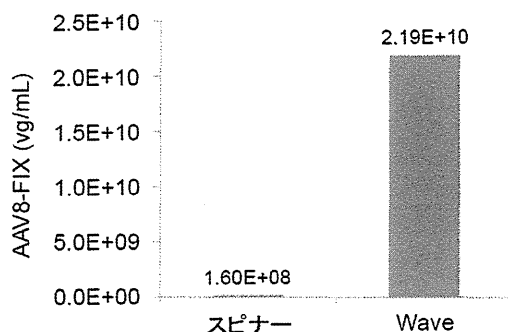


図8 スピナーフラスコと Wave 培養システムを用いた AAV ベクター大量製造検討

・新培地による AAV 産生効率上昇検討：現段階において、 $1 \times 10^{15} \text{vg}$ 製造ができるだけの基本的な条件は確立できたものと考えられるが、製造効率をさらに高めることができれば、ベクター純度、製造コストに大きく寄与できるため、タカラバイオで別途開発を行っていた昆虫細胞培養用培地について試験した (図 9)。

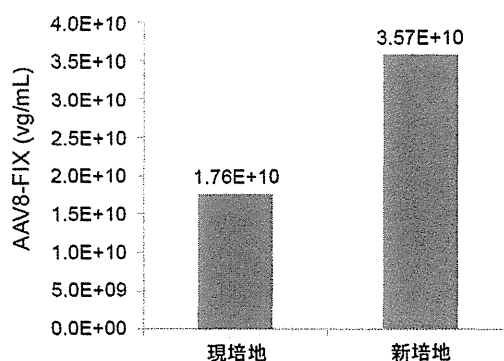


図9 開発中の新培地による AAV 産生効率

図 9 に示すように、予備試験段階の結果ではあるものの、新培地を用いることで、AAV 製造効率は約 2 倍に上昇した。

D. 考察

バキュロウイルスベクターを用いた AAV ベクター製造は、そのスケールアップの拡張性が高く、有望な技術ではあるが、その製造条件については相当の至適化が必要であった。また、AAV8-FIX ベクターを製造するにあたり、従来法であるヘルパーフリー法を検討した際に、FIX 遺伝子を搭載したベクターの産生効率が低いことが明らかとなっていたが、バキュロウイルスベクターを用いた場合においても同様に産生量の低下が認められた。しかしながら、臨床試

験に供するための製造量として 1×10^{15} vg を想定した場合に、種々の条件検討の結果、実際に製造可能なスケール (100-200L) での AAV ベクター製造のための条件を設定することができ、さらには実製造に使用予定の Wave Bioreactor を用いての検討においても同程度の効率での AAV ベクター産生性が確認できた。一方で、Sf9 MCB 製造において使用予定のスピナーフラスコにおいては、安定した細胞増殖が認められたものの、AAV ベクター産生効率は極端に悪く、おそらくは温度制御性の不安定性に起因するものと推察された。このことは、Wave Bioreactor での製造についても、不安定要因となりうることが考えられるが、細胞増殖性が安定しない中で実施した AAV ベクター製造試験において、一定の産生効率が確認できたことで、今後条件検討を進めることで、より安定で効率の高い製造条件を設定できる可能性も強く期待できた。なお、自治医科大学との協議により AAV8-FIX ベクターについてはできる限り早期に少数例での臨床試験を実施することになり、製造に時間を要するバキュロウイルスシステムではなく、従来法であるヘルパーフリー法により一定量のベクターを確保することとなった。そのため、今年度中に Sf9 昆虫細胞の MCB GMP 製造を実施する予定であったが、一旦とりやめ、ヘルパーフリー法に使用する pHelper プラスミドベクターの GMP 大量製造を実施中である (2/12 現在)。また、ベクター配列の見直し自治医科大学で実施され、余分な配列を除去した形で pAAV-FIX プラスミドベクターを人工合成した。さらに、以前の検討においてヘルパーフリー法では、例え少

数例であっても現状の製造条件では必要となるベクター量を確保することは難しいと見込まれるため、産生量を向上させるための検討を実施している。一方で、血友病 A に対する遺伝子治療用製剤となる AAV8-FVIII ベクターについては、症例も多いため、これまでの知見により確立されてきたバキュロウイルスシステムにより製造を行うこととなった。現在、自治医科大学でベクター配列の最終検討を実施中であり、完了次第、バキュロウイルスベクター製造用のトランスファーベクターへの載せ替えから実施する予定である。

E. 結論

本研究において、血友病 B に対する遺伝子治療臨床研究用ベクター製剤 AAV8-FIX の大量製造に関する検討を行った。昨年度の検討においてバキュロウイルスシステムの開発を進める結果が得られていたが、FIX 遺伝子を搭載することによるベクター製造効率の低下が確認された。そのため、種々の検討を行ったところ、実現可能なスケールでの AAV ベクター製造条件をある程度確定することができた。さらに、実製造で使用予定の Wave 培養システムによる製造効率ならびに Sf9 昆虫細胞 MCB GMP 製造のための条件についても確認できた。AAV8-FIX ベクターについては、方針の変更によりヘルパーフリー法により少数例分の製造を行うこととなったが、今後血友病 A に対する遺伝子治療用ベクターである AAV8-FIIIIV ベクター製造検討に本バキュロウイルスシステムを適用していく予定である。

G. 研究発表

Toshikazu Nishie, Tatsuji Enoki,
Masanari Kitagawa, Junichi Mineno,
Takashi Okada, Tsukasa Ohmori,
Hiroaki Mizukami, Keiya Ozawa, Yoichi
Sakata EXAMINATION ON LARGE
SCALE PRODUCTION OF AAV
VECTORS FOR CLINICAL USE, 日本遺
伝子治療学会, 2014年、東京

(発表誌名巻号・頁・発行年等も記入)

H. 知的財産権の出願・登録状況

なし

研究成果の刊行に関する一覧表

雑誌

発表者氏名	論文タイトル名	発表誌名	巻号	ページ	出版年
Sakata A, <u>Ohmori T</u> , Nishimura S, Suzuki H, <u>Madoiwa S</u> , Mimuro J, Kario K, <u>Sakata Y</u> .	Paxillin is an intrinsic negative regulator of platelet activation in mice.	Thromb J	12	1	2014
Koyama K, <u>Madoiwa S</u> , Nunomiya S, Koinuma T, Wada M, Sakata A, <u>Ohmori T</u> , Mimuro J, <u>Sakata Y</u> .	Combination of thrombin-antithrombin complex, plasminogen activator inhibitor-1, and protein C activity for early identification of severe coagulopathy in initial phase of sepsis: a prospective observational study.	Crit Care	18	R13	2014
Wada H, D. I. C. s. Japanese Society of Thrombosis Hemostasis, Okamoto K, Iba T, Kushimoto S, Kawasugi K, Gando S, <u>Madoiwa S</u> , Uchiyama T, Mayumi T, Seki Y.	Addition of recommendations for the use of recombinant human thrombomodulin to the "Expert consensus for the treatment of disseminated intravascular coagulation in Japan"	Thromb Res	134	924-925	2014
Sanada Y, Sasanuma H, Sakuma Y, Morishima K, N. Kasahara Y, Kaneda Y, Miki A, Fujiwara T, Shimizu A, Hyodo M, Hirata Y, Yamada N, Okada N, Ihara Y, Urahashi T, <u>Madoiwa S</u> , Mimuro J, K. Mizuta, Yasuda Y.	Living donor liver transplantation from an asymptomatic donor with mild coagulation factor IX deficiency: report of a case.	Pediatr Transplant	18	E270- E273	2014
Mimuro J, <u>Mizukami H</u> , <u>Shima M</u> , Matsushita T, <u>Taki M</u> , Muto S, Higasa S, Sakai M, <u>Ohmori T</u> , <u>Madoiwa S</u> , <u>Ozawa K</u> , <u>Sakata Y</u> .	The prevalence of neutralizing antibodies against adeno-associated virus capsids is reduced in young Japanese individuals.	J Med Virol	86	1990- 1997	2014
Chitlur M, Rivard GE, Lillicrap D, Mann K, <u>Shima M</u> , Young G: Factor VIII, Factor IX, and Rare Coagulation Disorders Subcommittee of the Scientific and Standardisation Committee of the International Society on Thrombosis and Haemostasis.	Recommendations for performing thromboelastography/thromboelastometry in hemophilia: communication from the SSC of the ISTH	Journal of Thrombosis and Haemostasis	12 (1)	103-106	2014

発表者氏名	論文タイトル名	発表誌名	巻号	ページ	出版年
Matsui H, Takeda M, Soejima K, Matsunari Y, Kasuda S, Ono S, Nishio K, <u>Shima M</u> , Banno F, Miyata T, Sugimoto M	Contribution of ADAMT S13 to the better cell engraftment efficacy in mouse model of bone marrow transplantation	Haematologica	99 (10)	e211-e213	2014
Matsui H, Fujimoto N, Sasakawa N, Ohinata Y, <u>Shima M</u> , Yamanka S, Sugimoto M, Hotta A.	Delivery of full-length factor VIII using a piggyBac transposon vector to correct a mouse model of hemophilia A	PLoS One	9(8)	e104957	2014
<u>Shima M</u> , Hermans C, de Moerloose P	Novel products for haemostasis	Haemophilia	20 (4)	29-35	2014
Yada K, Nogami K, Kawamura T, Minami H, <u>Shima M</u> .	The first case of interrelated inversion in Japanese haemophilia A patients	Haemophilia	20	e399-e443	2014
Matsumoto T, Nogami K, <u>Shima M</u> .	Coagulation function and mechanisms in various clinical phenotypes of patients with acquired factor V inhibitors	Journal of Thrombosis and Haemostasis	12 (9)	1503-1512	2014
Ogiwara K, Nogami K, Matsumoto T, <u>Shima M</u> .	Tissue factor pathway inhibitor in activated prothrombin complex concentrates (aPCC) moderates the effectiveness of therapy in some severe hemophilia A patients with inhibitor	International Journal of Hematology	99 (5)	577-587	2014
Nogami K, Shinozawa K, Ogiwara K, Matsumoto T, Amano K, Fukutake K, <u>Shima M</u> .	Novel FV mutation (W1920R, FVNara) associated with serious deep vein thrombosis and more potent APC resistance relative to FVLeiden	Blood	123 (15)	2420-2428	2014
Haku J, Nogami K, Matsumoto T, Ogiwara K, <u>Shima M</u> .	Optimal monitoring of bypass therapy in hemophilia A patients with inhibitors by the use of clot waveform analysis	Journal of Thrombosis and Haemostasis	12 (3)	355-362	2014

発表者氏名	論文タイトル名	発表誌名	巻号	ページ	出版年
Isshiki M, Zhang X, Sato H, Ohashi T, <u>Inoue M</u> , Shida H.	Effects of different promoters on the virulence and immunogenicity of a HIV-1 Env-expressing recombinant vaccinia vaccine.	Vaccine	32(7)	839-845	2014
Nagao A, Hanabusa H, <u>Takedani H</u> .	Continuous infusion of rFVIIa during surgery in a FVII-deficient patient: a case report from Japan.	Haemophilia	20(1)	e110-e112	2014
Goto M, <u>Takedani H</u> , Haga N, Kubota M, Ishiyama M, Ito S, Nitta O.	Self-monitoring has potential for home exercise programmes in patients with haemophilia.	Haemophilia	20(2)	e121-e127	2014
Shimokawa A, <u>Takedani H</u> .	Rehabilitation improved walking ability for three haemophilia patients with inhibitors.	Haemophilia	20(3)	e222-e224	2014
Miyamoto Y, Iida A, Sato K, <u>Muramatsu S</u> , Nitta A.	Knockdown of dopamine D2 receptors in the nucleus accumbens core suppresses methamphetamine-induced behaviors and signal transduction in mice.	Int JNP		In press	2014
Miyamoto Y, Ishikawa Y, Iegaki N, Sumi K, Fu K, Sato K, Furukawa-Hibi Y, <u>Muramatsu S</u> , Nabeshima T, Uno K, Nitta A.	Overexpression of Shat1/Nat8l, an N-acetyltransferase, in the nucleus accumbens attenuates the response to methamphetamine via activation of group II mGluRs in mice.	Int J Neuropsychopharmacol	17	1283-1294	2014
Ito H, Fujita K, Tagawa K, Chen X, Homma H, Sasabe T, Shimizu J, Shimizu S, Tamura T, <u>Muramatsu S</u> Okazawa H.	HMGB1 facilitates repair of mitochondrial DNA damage and extends the lifespan of mutant taxin-1 knock-in mice.	EMBO Mol Med	7(1)	78-101	2014

研究成果の刊行物・別刷

ORIGINAL BASIC RESEARCH

Open Access

Paxillin is an intrinsic negative regulator of platelet activation in mice

Asuka Sakata^{1,2}, Tsukasa Ohmori^{1*}, Satoshi Nishimura^{1,3,4}, Hidenori Suzuki⁵, Seiji Madoiwa¹, Jun Mimuro¹, Kazuomi Kario² and Yoichi Sakata¹

Abstract

Background: Paxillin is a LIM domain protein localized at integrin-mediated focal adhesions. Although paxillin is thought to modulate the functions of integrins, little is known about the contribution of paxillin to signaling pathways in platelets. Here, we studied the role of paxillin in platelet activation *in vitro* and *in vivo*.

Methods and results: We generated paxillin knockdown (Pxn-KD) platelets in mice by transplanting bone marrow cells transduced with a lentiviral vector carrying a short hairpin RNA sequence, and confirmed that paxillin expression was significantly reduced in platelets derived from the transduced cells. Pxn-KD platelets showed a slight increase in size and augmented integrin $\alpha\text{IIb}\beta\text{3}$ activation following stimulation of multiple receptors including glycoprotein VI and G protein-coupled receptors. Thromboxane A_2 biosynthesis and the release of α -granules and dense granules in response to agonist stimulation were also enhanced in Pxn-KD platelets. However, Pxn-KD did not increase tyrosine phosphorylation or intracellular calcium mobilization. Intravital imaging confirmed that Pxn-KD enhanced thrombus formation *in vivo*.

Conclusions: Our findings suggest that paxillin negatively regulates several common platelet signaling pathways, resulting in the activation of integrin $\alpha\text{IIb}\beta\text{3}$ and release reactions.

Keywords: Platelet, Glycoprotein, Platelet aggregation, Release reaction

Background

A breakdown of normal platelet function results in either unexpected bleeding or thrombotic events [1]. Platelets are inactive in the intact vasculature under physiological conditions. However, once the platelets encounter an injured region of the endothelium, they attach through an interaction between von Willebrand factor and the glycoprotein (GP) Ib/IX/V complex [2], and then collagen receptor GPVI triggers platelet activation. Activated platelets release several classes of agonists, including ADP and thromboxane (Tx) A_2 , which promote further platelet activation [3]. These steps ultimately increase the affinity of integrin $\alpha\text{IIb}\beta\text{3}$ for its ligands and induce platelet aggregation [4]. The intracellular signaling that increases the affinity of integrins is known as inside-out signaling [4]. Multiple signal transduction pathways from various

receptors share common inside-out signaling cascades. For example, phosphoinositol hydrolysis, which leads to calcium mobilization and protein kinase C activation [5], and Rap1b activation are well-known signaling pathways that regulate integrin-mediated platelet functions [6].

To increase the affinity of integrin $\alpha\text{IIb}\beta\text{3}$, inside-out signaling pathways induce a drastic conformational change of the integrin [7]. Direct interactions between cytoskeletal proteins (e.g., talin and kindlin) and cytoplasmic β integrin are essential for inducing the conformational change of integrins [7]. Indeed, the loss of talin or kindlin in platelets dramatically reduces integrin $\alpha\text{IIb}\beta\text{3}$ -mediated platelet aggregation, despite normal expression levels of the surface receptors [8,9]. Selective blockade of talin binding by a single amino acid substitution in β3 integrin also impairs integrin $\alpha\text{IIb}\beta\text{3}$ -dependent platelet responses [10]. Although a number of integrin-associated proteins have been reported [11], the identities of proteins and their roles in regulating integrin signaling in platelets have not been fully characterized. It is also unknown whether

* Correspondence: tohmori@jichi.ac.jp

¹Research Division of Cell and Molecular Medicine, Center for Molecular Medicine, Jichi Medical University School of Medicine, 3111-1 Yakushiji, Shimotsuke, Tochigi 329-0498, Japan

Full list of author information is available at the end of the article



additional molecules, other than talin and kindlin, are capable of regulating integrin signaling pathways.

Paxillin is a LIM domain protein that was originally identified as a substrate for oncogene *v-src* [12]. Paxillin contains two conserved structural domains, the N-terminus and C-terminus, which consist of four LIM domains [13,14]. Two other family members have also been identified, Hic-5 and leupaxin [13,14]. Paxillin is ubiquitously expressed alongside these variants [13,14], except in human platelets that predominantly express Hic-5 [15,16]. Conversely, mouse platelets express paxillin and leupaxin in addition to Hic-5 [17]. Considering the multiple interaction motifs located within its structure, paxillin appears to serve as a signaling platform for the recruitment of numerous regulatory proteins near integrins [13,14]. Paxillin directly interacts with the cytoplasmic domain of integrin $\alpha 4$ and $\alpha 9$, but not $\alpha 1b$, and these interactions control integrin-mediated cell migration and spreading [18,19].

Integrin $\alpha 1b\beta 3$ in platelets is suitable for studies of integrin receptors because its ligand binding and signal transduction pathways are well characterized. Elucidating the intracellular proteins involved in the activation of integrin $\alpha 1b\beta 3$ can provide a better understanding of the functions of integrins and might result in the discovery of new antithrombotic targets [20]. We previously reported that lentiviral vector-mediated short hairpin RNA (shRNA) expression in hematopoietic stem cells greatly reduces the expression of the target protein in platelets [21]. This method enables functional analyses of target proteins that modulate platelet activation in anucleate platelets [21]. In the present study, we used this method to investigate the roles of paxillin in platelet activation, and found that paxillin negatively regulates platelet signaling pathways including the activation of integrin $\alpha 1b\beta 3$ and release reactions.

Materials and methods

Materials

All mouse cytokines were purchased from PeproTech (London, UK). The following antibodies and agonists were obtained from the specified suppliers: PAC-1 monoclonal antibody (mAb), anti-mouse P-selectin mAb (RB40.34), anti-paxillin mAb (clone 349), and anti-Hic-5 mAb (BD Biosciences, San Jose, CA); horseradish peroxidase-conjugated anti-green fluorescent protein (GFP) polyclonal antibody (Acris Antibodies, Himmelreich, Germany); phycoerythrin (PE)-Cy7-conjugated anti-mouse IgM (eBioscience, San Diego, CA); anti-talin mAb (clone 8D4); anti-phosphotyrosine mAb (clone 4G10), and BAPTA-AM (Millipore, Billerica MA); human fibrinogen and epinephrine (Sigma-Aldrich, St. Louis, MO); anti-vinculin mAb (V284) (Chemicon, Billerica, MA); anti-mouse GPVI mAb (Six.E10), anti-mouse GPIb α mAb (Xia.G5), and anti-mouse integrin $\alpha 1b\beta 3$ mAb (Leo.D2 and clone

JON/A) (Emfret Analytics, Eibelstadt, Germany); anti- α -actin mAb (D6F6), anti-FAK polyclonal antibody, and anti-Src mAb (32G6) (Cell Signaling Technology, Danvers, MA); anti-Rap1b polyclonal antibody and anti-protein kinase C α mAb (M4) (Upstate Cell Signaling Solutions, Lake Placid, NY); allophycocyanin (APC)-conjugated anti-rat IgG polyclonal antibody (R& D Systems, Minneapolis, MN); convulxin (ALEXIS Biochemicals, Plymouth Meeting, PA); AYPGKF (Invitrogen, Carlsbad, CA); ADP (MC medical, Tokyo, Japan); U46619 (Cayman Chemical, Ann Arbor, MI).

Lentiviral vector and virus production

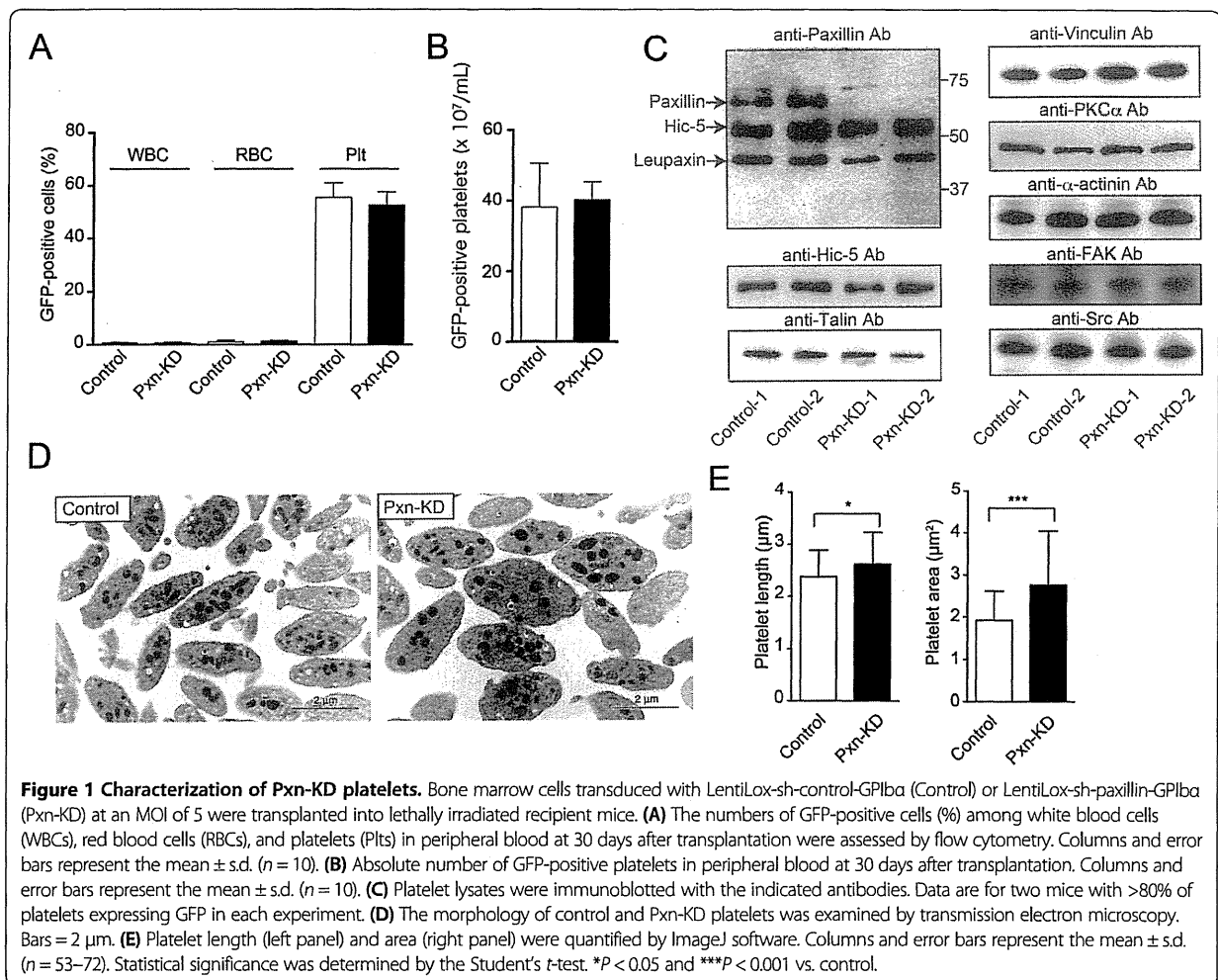
A lentiviral vector plasmid for expression of shRNA sequences and GFP (LentiLox vector) was purchased from the American Type Culture Collection (Manassas, VA) [22]. To efficiently express GFP in platelets, the cytomegalovirus promoter of the LentiLox vectors was substituted with the platelet-specific GPIb α promoter (LentiLox-GPIb α) [21]. Putative shRNA sequences were designed using web-based software provided by Thermo Scientific Molecular Biology (<http://www.thermoscientificbio.com/design-center/>). Three shRNA sequences were synthesized for mouse paxillin and then cloned into a LentiLox vector plasmid (Additional files 1 and 2). Lentiviruses were produced as described previously [23].

Transplantation of mouse bone marrow cells

All animal procedures were approved by the Institutional Animal Care and Concern Committee of Jichi Medical University, and animal care was performed in accordance with the committee's guidelines. Mouse bone marrow cells (C57BL/6 J) were isolated and resuspended in StemPro[®]-34 SFM medium (Invitrogen) supplemented with 100 ng/mL each of stem cell factor, thrombopoietin, interleukin-6, and fms-like tyrosine kinase 3 ligand, and 200 ng/mL soluble interleukin-6 receptor. The lentiviral vector was added at 12–16 h after cell isolation (multiplicity of infection [MOI] = 5), and the cell culture was continued for 21–22 h. Each recipient mouse (8–12 weeks of age) was irradiated with a single lethal dose of 9.5 Gy and then intravenously injected with 2×10^6 lentivirus-transduced bone marrow cells. After transplantation, about 50% of platelets expressed GFP (Figure 1). Mice with 70% of their platelets exhibiting GFP positivity were used in experiments that could not distinguish GFP-positive platelets, *i.e.*, light transmission aggregometry, clot retraction, release concentration, calcium mobilization, and intravital microscopy.

Immunoblotting

Immunoblotting with the specific antibodies was performed as described previously [21]. To assess protein tyrosine phosphorylation, washed platelets were pretreated



with 1 mmol/L EDTA, 5 U/mL apyrase, and 10 μmol/L SQ29548 to exclude the effects of aggregation, released ADP, and TxA₂.

Transmission electron microscopy

Mouse platelet pellets were fixed in 2% glutaraldehyde in 0.1 mol/L phosphate buffer (pH 7.4) for 60 min at 4°C. The samples were washed, post-fixed with 1% osmium tetroxide in 0.1 mol/L phosphate buffer for 60 min at 4°C, dehydrated with a graded ethanol series, and then embedded in Epon (TAAB Laboratories, Aldermaston, UK) as described previously [24]. Ultrathin sections were prepared, stained with uranyl acetate and lead citrate, and then examined under a JEM1010 transmission electron microscope (JEOL, Tokyo, Japan) at an accelerating voltage of 80 kV. The length and area of platelets were quantified using ImageJ Ver. 10.2 for Macintosh (NIH, Bethesda, MD).

Preparation of washed mouse platelets and flow cytometry

A blood sample (100–400 μL) was drawn from each mouse through the right jugular vein using a 30 G syringe containing 1/10 sodium citrate, and then diluted with 3 mL Hepes/Tyrode buffer (138 mmol/L NaCl, 3.3 mmol/L NaH₂PO₄, 2.9 mmol/L KCl, 1 mmol/L MgCl₂, 1 mg/mL glucose, and 20 mmol/L Hepes, pH 7.4). The diluted blood was centrifuged at 120 × g for 8 min, and the platelets obtained from the platelet-rich fraction were washed and resuspended in Hepes/Tyrode buffer. Just prior to centrifugation, a 15% acid-citrate-dextrose A solution and 0.1 μmol/L prostaglandin I₂ were added to inhibit platelet activation. The final platelet suspensions were adjusted to 1 × 10⁷ platelets/mL and supplemented with 1 mmol/L CaCl₂. To assess the binding of JON/A, a monoclonal antibody (mAb) that recognizes activated mouse αIIbβ3 [25], to platelets, 30 μL of washed platelets was incubated with 4 μL of agonist solution, 4 μL of phycoerythrin (PE)-

conjugated JON/A and 1 μ L of biotin-conjugated anti-mouse P-selectin mAb for 5 min, and then supplemented with 1 μ L of allophycocyanin (APC)-conjugated streptavidin. After 15 min of incubation, JON/A binding and P-selectin expression were determined by flow cytometry using a FACSAria Cell Sorter (Becton Dickinson, Mountain View, CA). Antibody binding was quantified as the mean fluorescence intensity (MFI) of GFP-positive platelets.

Platelet aggregation

Washed platelets were prepared as described above. The final suspensions were adjusted to 2×10^8 platelets/mL and supplemented with 1 mmol/L CaCl_2 and 200 μ g/mL fibrinogen. The aggregation response to agonist stimulation was measured based on light transmission measured using a PA-200 platelet aggregation analyzer (Kowa, Tokyo, Japan).

Measurement of platelet products

Washed platelets (2×10^8 /mL) were stimulated with the indicated agonists for 15 min, and then the supernatants were recovered by centrifugation. The levels of platelet factor 4 (PF4) and serotonin in the supernatants were measured using a mouse PF4 enzyme-linked immunosorbent assay (ELISA) kit (R & D Systems) and an anti-serotonin ELISA kit (GenWay Biotech, San Diego, CA), respectively. The levels of TxB_2 in the supernatants were measured using an enzyme immunoassay (Cayman Chemical).

Platelet adhesion

Platelet adhesion to fibrinogen was assessed as described previously [21]. Briefly, eight-well dishes (Lab-Tek[®] Chamber Slide[™]) were coated with 400 μ g/mL fibrinogen and then blocked with 1 mg/mL bovine serum albumin (BSA). Platelets were then added to the fibrinogen-coated dishes and incubated for 30 min at 37°C. Adherent platelets were fixed with 3% paraformaldehyde and then permeabilized with phosphate-buffered saline (PBS) containing 0.3% Triton X-100 and 5% donkey serum. After washing with PBS, the platelets were incubated with an anti-GFP polyclonal antibody (MBL, Aichi, Japan). Bound antibodies were detected by Alexa Fluor 488-conjugated anti-rabbit IgG. Actin filaments were detected by staining with 1 μ g/mL rhodamine-conjugated phalloidin. Immunofluorescence staining was observed and photographed under a confocal microscope (FV1000; Olympus, Tokyo, Japan). The spread area of GFP-positive platelets was quantified using ImageJ software. Because Pxn-KD platelets were slightly larger than control platelets (Figure 1), the mean platelet size determined by BSA staining was subtracted from the total area on fibrinogen to calculate the actual increase in platelet spreading.

Clot retraction

Human platelet-poor plasma was mixed with the same volume of HEPES/Tyrode buffer containing washed mouse platelets (final concentration: 3×10^8 platelets/mL). Plasma coagulation was initiated by addition of 0.1 U/mL thrombin. The clots were photographed at various time points after thrombin addition. When indicated, 0.5 mmol/L manganese was added to exclude the role of inside-out signaling. The two-dimensional area of serum formation extruded by clot retraction was quantified using ImageJ software and expressed as the progression of clot retraction.

Calcium mobilization

Platelets were incubated with GFP-Certified[™] FluoForte[™] dye (Enzo Life Sciences, Farmingdale, NY). The fluorophore-loaded platelets (2×10^8 /mL) were resuspended in HEPES-Tyrode buffer containing 1 mmol/L EDTA, 5 U/mL apyrase, and 10 μ mol/L SQ29548 to exclude the effects of aggregation, extracellular calcium, released ADP, and TxA_2 . After stimulation, the intracellular calcium concentration was determined by monitoring the fluorescence (excitation, 530 nm; emission, 570 nm) using a microplate spectrofluorometer (Gemini EM; Molecular Devices, Sunnyvale, CA).

Intravital microscopy and thrombus formation

Intravital microscopy was performed to analyze thrombus formation *in vivo* as reported previously [26]. Briefly, Texas Red-dextran (100 mg/kg body weight [BW], molecular weight: 70 kDa; Invitrogen, Hoechst 33342 (10 mg/kg BW; Invitrogen), Dylight 488-conjugated anti-CD42b antibody (200 μ g/kg BW; Emfret), and hematoporphyrin (5 mg/kg BW; Sigma) were injected into anesthetized mice to produce reactive oxygen species (ROS) following laser irradiation. Blood cell dynamics were visualized during laser excitation (wavelengths 405, 488, and 561 nm; 1.5 mW total power at 100 \times objective lens). After laser irradiation, sequential images of the mesentery were obtained using a resonance scanning confocal microscope (Nikon A1R; Nikon, Tokyo, Japan). The areas of thrombus (shown by anti-CD42b antibody signals) before and after laser irradiation were calculated using NIS-Elements AR 3.2 (Nikon). When indicated, thrombus formation in the femoral artery was triggered by topical application of a filter paper tip saturated with 10% FeCl_3 . After injection of Texas Red-dextran, Hoechst 33342, and Dylight 488-conjugated anti-CD42b antibody, thrombus formation was visualized and monitored by confocal microscopy using two photon microscopy (excitation wavelength 840 nm) by Nikon A1R MP (Nikon).

Bleeding time

The distal tail tip (5 mm) of an anesthetized mouse was clipped, and the tail was immediately immersed in PBS

at 37°C. Tail bleeding times were defined as the time required for the bleeding to stop.

Results

Generation of paxillin knockdown (Pxn-KD) platelets

To address the function of paxillin in mouse platelets, we used a lentiviral vector carrying shRNA sequences and GFP [22]. We synthesized three shRNA sequences for mouse paxillin, and cloned them into a LentiLox vector plasmid (Additional files 1 and 2). We selected one sequence that significantly inhibited paxillin expression in embryonic fibroblasts after transduction (Pxn-1 sequence; Additional files 1 and 2). After transplantation of bone marrow cells transduced with either the control or Pxn-KD sequence, about 50% of the platelets expressed GFP, and the absolute numbers of GFP-positive platelets did not differ between experiments using control and Pxn-KD sequences (Figure 1A–B). Furthermore, there was no effect on the total number of platelets (control: $6.8 \pm 1.72 \times 10^8/\text{mL}$; Pxn-KD: $7.7 \pm 0.65 \times 10^8/\text{mL}$, $P = 0.18$). We compared the platelet aggregation response and release reaction in platelets from wild-type C57BL/6 J and control mice, and confirmed that platelet aggregation as well as the release reaction did not differ (data not shown). To confirm knockdown of paxillin in GFP-positive platelets, we selected mice in which more than 80% of platelets expressed GFP after transplantation. Immunoblotting of platelet lysates with an anti-paxillin mAb (clone 349) showed a marked reduction in paxillin expression following transplantation of bone marrow cells transduced with the Pxn-KD sequence (Figure 1C). This antibody also recognizes other members of the paxillin family, including Hic-5 and leupaxin [17]. However, Hic-5 and leupaxin were not affected by expression of the Pxn-KD sequence (Figure 1C). Transmission electron microscopy of resting platelets revealed that the Pxn-KD platelets were slightly larger than control platelets (Figure 1D–E). This change was largely dependent on an increase of the cytoplasm volume, but not the granule volume (Additional file 3). Pxn-KD platelets showed marginally elevated expression levels of GPIb and integrin $\alpha\text{IIb}\beta_3$, even though GPVI expression was normal (Additional file 4). These changes in Pxn-KD platelets were supposed to result from the increase in platelet size.

Augmentation of integrin $\alpha\text{IIb}\beta_3$ activation in Pxn-KD platelets

We first focused on the role of paxillin in integrin $\alpha\text{IIb}\beta_3$ activation that is critical for platelet aggregation. We performed flow cytometric analysis of integrin $\alpha\text{IIb}\beta_3$ activation using an anti-JON/A mAb [25]. GFP-positive Pxn-KD platelets (Figure 2A, lower panel) showed significantly enhanced $\alpha\text{IIb}\beta_3$ activation following stimulation compared with that of control platelets (Figure 2A, upper panel).

Enhanced JON/A binding of Pxn-KD platelets was observed following stimulation with the GPVI agonist convulxin and G protein-coupled receptor agonists including a protease-activated receptor 4 agonist (AYPGKF), ADP, and U46619 (Figure 2A–B). However, JON/A binding was not enhanced in unstimulated or epinephrine-stimulated platelets, suggesting that Pxn-KD alone does not induce activation of integrin $\alpha\text{IIb}\beta_3$. We next used light transmission aggregometry to assess platelet aggregation *in vitro*. We found that platelet aggregation was significantly augmented in Pxn-KD platelets, and this effect was evident at low agonist concentrations that induce platelet aggregation (Figure 2C–D).

Enhanced release reactions and Tx biosynthesis in Pxn-KD platelets

We next assessed the release reactions in response to stimulation. To address the role of paxillin in α -granule secretion, P-selectin expression was determined in GFP-positive platelets by flow cytometry. As shown in Figure 3A–B, P-selectin expression in Pxn-KD platelets was significantly increased following stimulation with convulxin, AYPGKF, and U46619. In contrast, P-selectin expression was not increased by stimulation with ADP or epinephrine. We observed negligible increases in P-selectin expression of Pxn-KD platelets under the resting condition and after incubation with the fibronectin peptide Gly-Arg-Gly-Asp-Ser (GRGDS) (Figure 3B). To examine whether Pxn-KD platelets are already activated during circulation, we compared P-selectin expression in washed platelets and whole blood platelets before the preparation. An increase of P-selectin expression after washing the platelet preparation was observed in Pxn-KD platelets (30.0 ± 9.71 to 37.2 ± 5.72 in the control vs. 27.8 ± 2.56 to 44.8 ± 7.87 , $P < 0.05$), suggesting that the susceptibility of Pxn-KD platelets caused marginal activation during washing. Although PF4 and serotonin content in resting platelets did not differ between control and Pxn-KD platelets (Additional file 3), the actual release of PF4 and serotonin into the supernatant in response to platelet activation was also enhanced in Pxn-KD platelets (Figure 3C–D). Of note, a marked increase in TxB_2 biosynthesis was observed in Pxn-KD platelets (Figure 3E). Pretreatment with the ADP scavenger apyrase and thromboxane A_2 receptor antagonist SQ29548 somewhat corrected the increase of JON/A binding in Pxn-KD platelets. This result suggests that the extent of the increase of integrin activation is partially dependent on the release reaction (Additional file 5). Collectively, these data suggest that paxillin negatively regulates platelet activation signaling pathways leading to integrin activation, release reactions, and Tx synthesis. It is possible that general pathway(s) involved in platelet activation were enhanced by Pxn-KD, because platelet activation was increased in

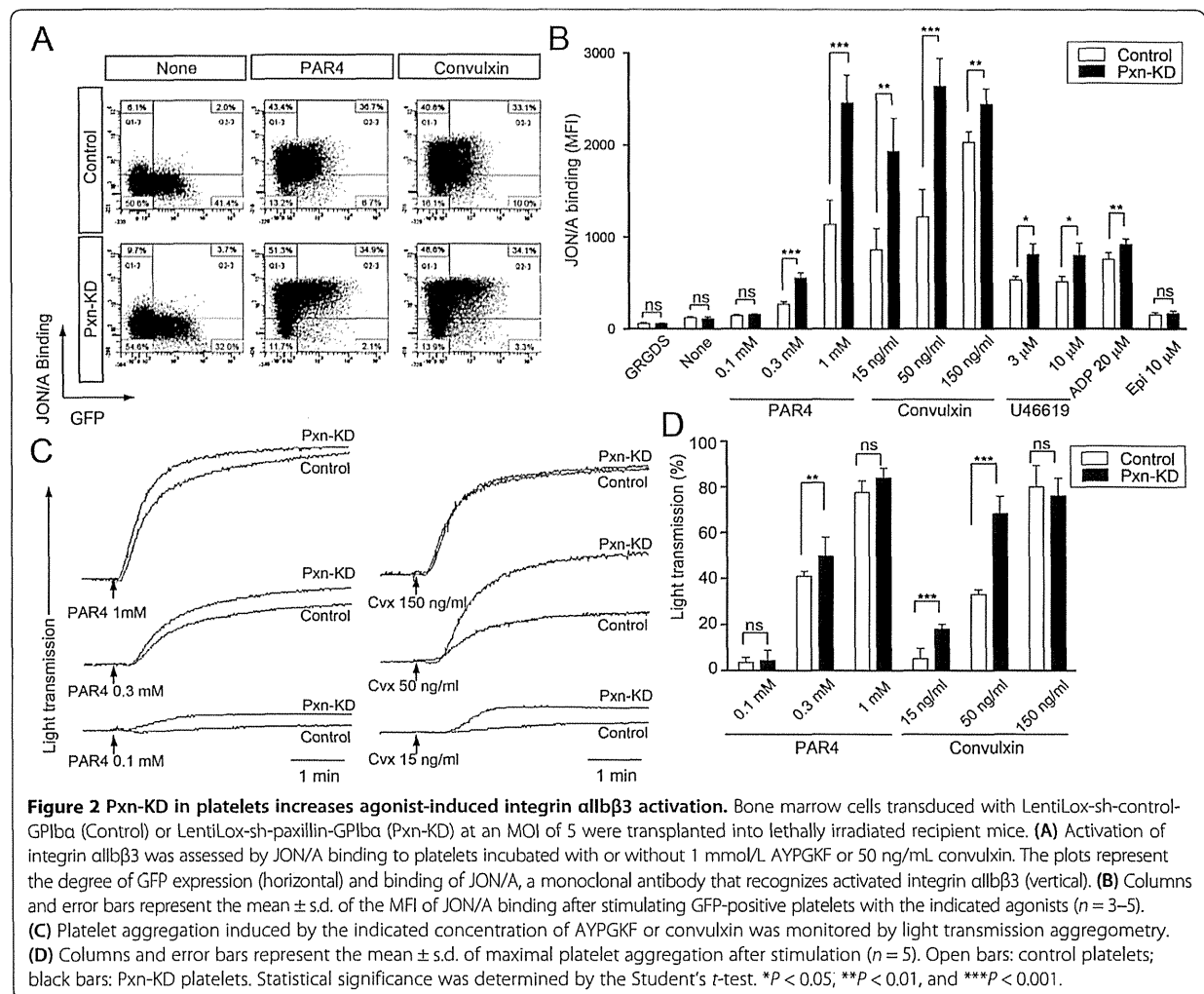


Figure 2 Pxn-KD in platelets increases agonist-induced integrin α IIb β 3 activation. Bone marrow cells transduced with LentiLox-sh-control-GPIIb α (Control) or LentiLox-sh-paxillin-GPIIb α (Pxn-KD) at an MOI of 5 were transplanted into lethally irradiated recipient mice. (A) Activation of integrin α IIb β 3 was assessed by JON/A binding to platelets incubated with or without 1 mmol/L AYPGKF or 50 ng/mL convulxin. The plots represent the degree of GFP expression (horizontal) and binding of JON/A, a monoclonal antibody that recognizes activated integrin α IIb β 3 (vertical). (B) Columns and error bars represent the mean \pm s.d. of the MFI of JON/A binding after stimulating GFP-positive platelets with the indicated agonists ($n = 3-5$). (C) Platelet aggregation induced by the indicated concentration of AYPGKF or convulxin was monitored by light transmission aggregometry. (D) Columns and error bars represent the mean \pm s.d. of maximal platelet aggregation after stimulation ($n = 5$). Open bars: control platelets; black bars: Pxn-KD platelets. Statistical significance was determined by the Student's *t*-test. * $P < 0.05$, ** $P < 0.01$, and *** $P < 0.001$.

response to several classes of activators including GPVI and G protein-coupled receptors.

Assessment of outside-in signaling pathways in Pxn-KD platelets

To address the role of paxillin in outside-in signaling of integrin α IIb β 3, we assessed platelet spreading on fibrinogen and clot retraction. The cell area independent of integrin outside-in signaling (i.e., adherent to the BSA control) was slightly increased in Pxn-KD platelets compared with that in control platelets (data not shown), because the Pxn-KD platelets were marginally larger than control platelets (Figure 1). To quantify the increase in platelet spreading, the mean platelet size on BSA was subtracted from the total spreading area on fibrinogen. As shown in Figure 4A, the increase in platelet spreading on fibrinogen without or with convulxin stimulation was significantly greater for Pxn-KD platelets than that for control platelets (Figure 4A-B). In addition, clot retraction

induced by thrombin was significantly enhanced in Pxn-KD platelets compared with that in control platelets (Figure 4C-D). Acceleration of clot retraction in Pxn-KD platelets was also observed in the presence of manganese at 15 min (6.98 ± 0.130 vs. 7.56 ± 0.072 , $P < 0.05$). These observations suggest that paxillin is an important regulator of integrin outside-in signaling via integrin α IIb β 3.

The role of paxillin in calcium mobilization in platelets

Because GPVI initiates signaling cascades by activation of non-receptor tyrosine kinases, we assessed tyrosine phosphorylation elicited by the GPVI signaling pathway. As a result, tyrosine phosphorylation events induced by convulxin were not affected by Pxn-KD (Figure 5A). The agonist-induced increase in intracellular calcium mobilization is an important common and proximal signaling event controlling platelet activation. Therefore, we next examined whether Pxn-KD enhanced intracellular calcium mobilization following stimulation. To exclude

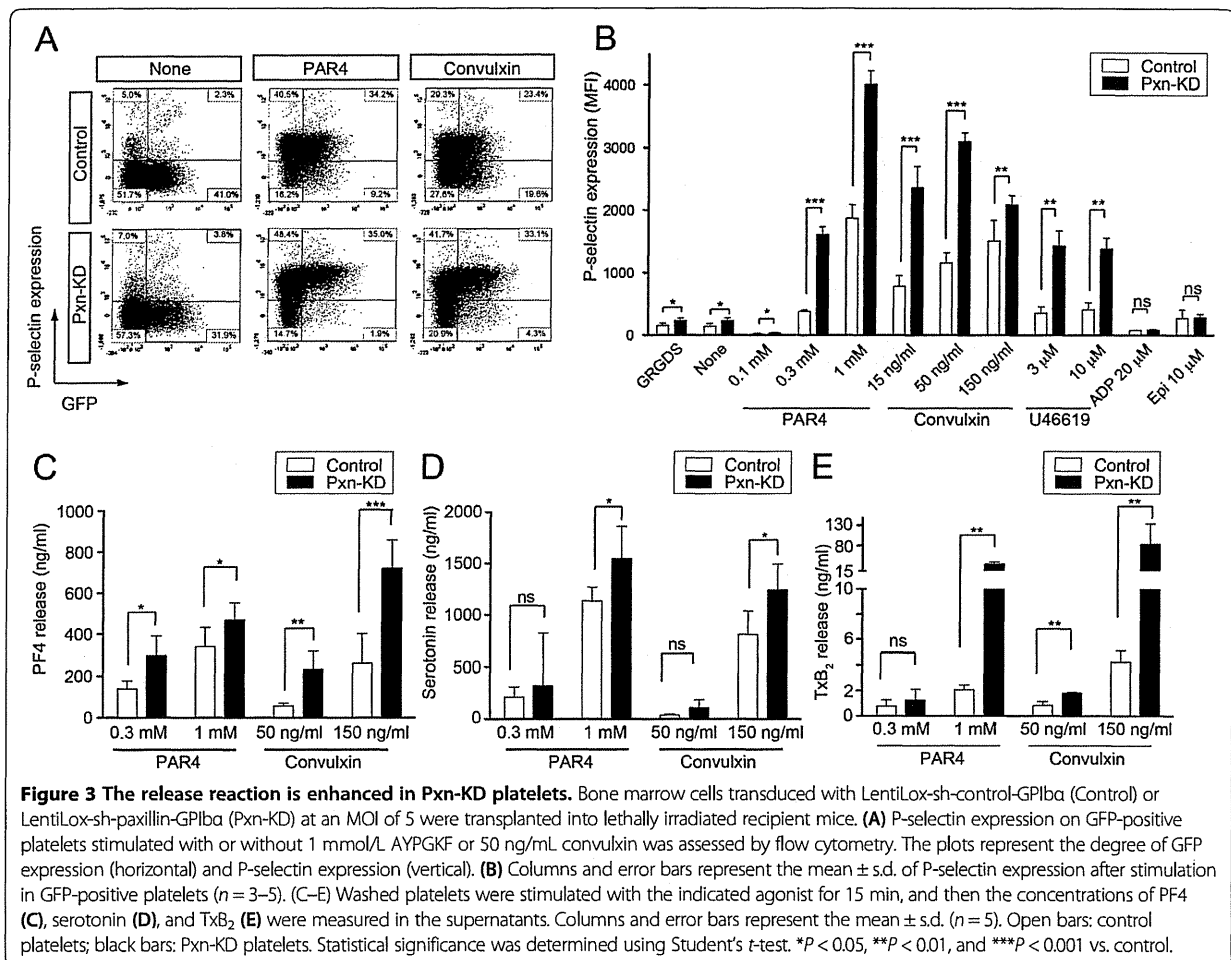


Figure 3 The release reaction is enhanced in Pxn-KD platelets. Bone marrow cells transduced with LentiLox-sh-control-GPIIbα (Control) or LentiLox-sh-paxillin-GPIIbα (Pxn-KD) at an MOI of 5 were transplanted into lethally irradiated recipient mice. **(A)** P-selectin expression on GFP-positive platelets stimulated with or without 1 mmol/L AYPGKF or 50 ng/mL convulxin was assessed by flow cytometry. The plots represent the degree of GFP expression (horizontal) and P-selectin expression (vertical). **(B)** Columns and error bars represent the mean ± s.d. of P-selectin expression after stimulation in GFP-positive platelets ($n = 3-5$). **(C-E)** Washed platelets were stimulated with the indicated agonist for 15 min, and then the concentrations of PF4 **(C)**, serotonin **(D)**, and TxB₂ **(E)** were measured in the supernatants. Columns and error bars represent the mean ± s.d. ($n = 5$). Open bars: control platelets; black bars: Pxn-KD platelets. Statistical significance was determined using Student's *t*-test. * $P < 0.05$, ** $P < 0.01$, and *** $P < 0.001$ vs. control.

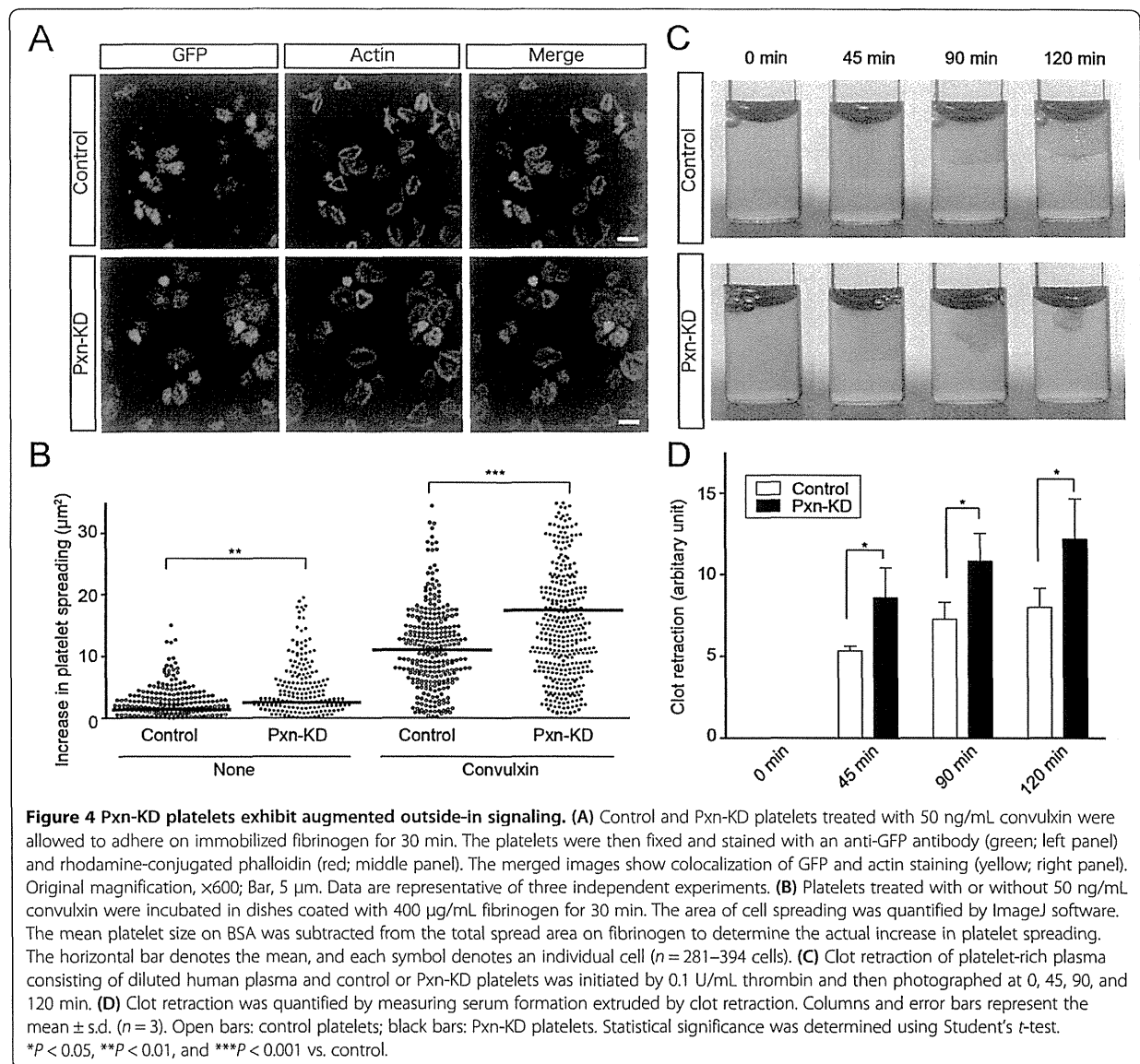
secondary effects of platelet aggregation, influx of extracellular calcium, and release reactions, we preincubated the platelets with EDTA, apyrase, and SQ29548. Intracellular calcium mobilization induced by the GPVI agonist convulxin and G protein-coupled receptor stimulation with AYPGKF was rather decreased by Pxn-KD (Figure 5B). These data suggest that paxillin targets downstream signaling of calcium mobilization or a calcium-independent signaling pathway.

To explore the importance of calcium-independent signaling pathways in Pxn-KD platelets, we employed BAPTA-AM, an intracellular calcium chelator, to exclude the effect of calcium mobilization. Because JON/A requires extracellular calcium for antibody binding, we assessed P-selectin expression induced by an agonist. Pretreatment with BAPTA-AM significantly suppressed P-selectin expression in both control and Pxn-KD platelets (Figure 5C). On the other hand, P-selectin expression elicited by an agonist was still observed in Pxn-KD platelets even in the presence of BAPTA-AM (Figure 5C).

These data indicate that downstream signaling from intracellular calcium mobilization is amplified by Pxn-KD, and the calcium-independent pathway is activated by Pxn-KD to increase platelet activation.

Pxn-KD augments platelet adhesion and thrombus formation in vivo

Finally, we examined the contribution of paxillin to thrombus formation in vivo. To visualize thrombus formation in vivo, we used a direct visual technique based on confocal microscopy in mesenteric capillaries [26]. Thrombus formation in this system was initiated by the production of ROS following laser irradiation [26]. Laser irradiation-induced thrombus formation was significantly enhanced in Pxn-KD platelets (Figure 6A and 6B and Additional files 6 and 7). In addition, there was an enhancement of thrombus formation initiated by FeCl₃ in large femoral arteries (Additional file 8). Moreover, bleeding times after tail clipping significantly shortened in Pxn-KD experiments (Figure 6C). These findings support



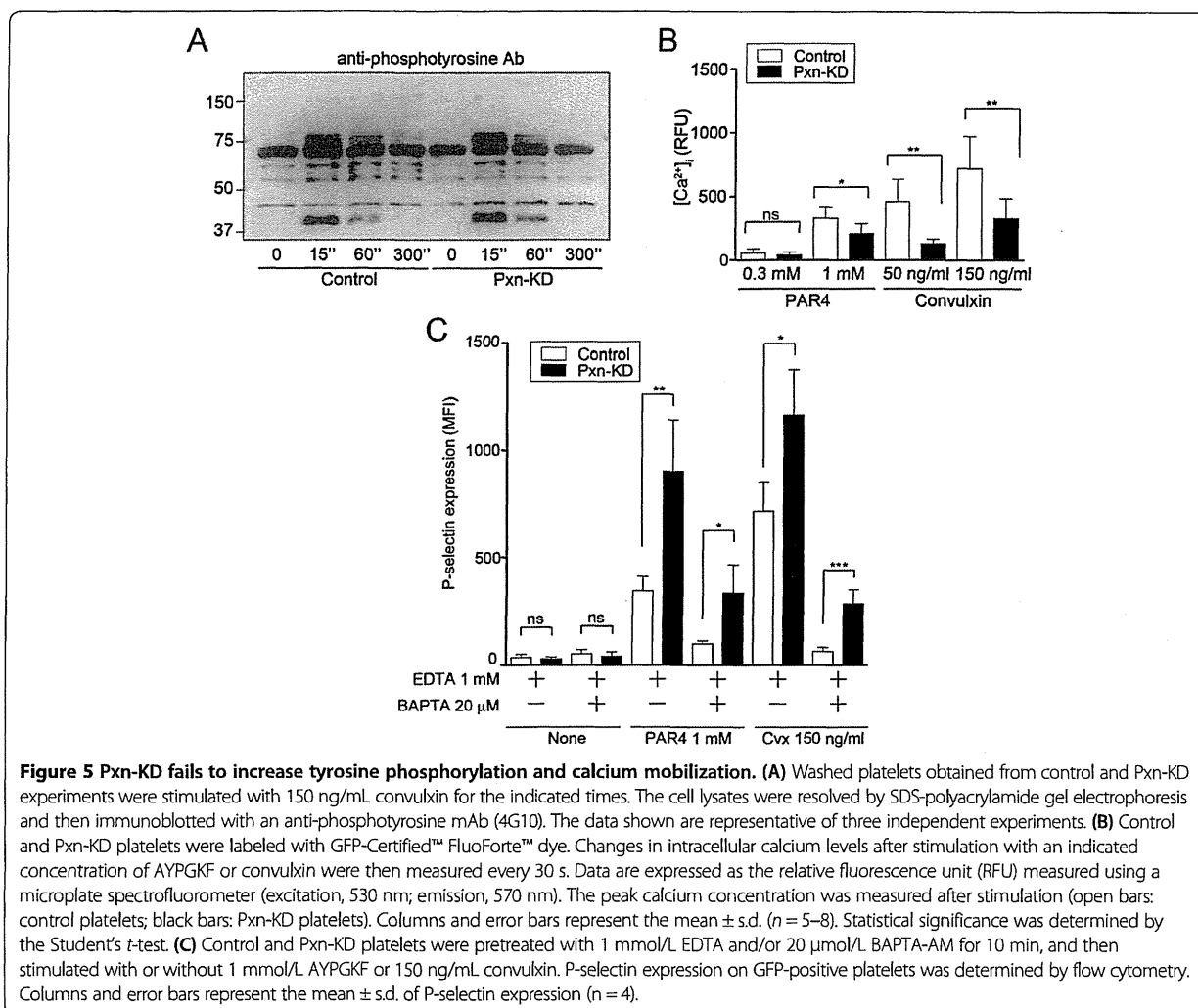
our hypothesis that paxillin is an important negative regulator of platelet activation and thrombus formation in vivo.

Discussion

Here, we found that the LIM protein paxillin is a negative regulator of platelet activation in mice. The negative regulation of platelet activation by paxillin was not limited to a specific signaling pathway, because Pxn-KD enhanced platelet activation in response to a variety of agonists. We also confirmed that thrombus formation was augmented in Pxn-KD platelets in vivo. This finding is notable because several previous reports suggest that changes in paxillin function actually reduce integrin signaling [13,14]. Furthermore, a previous finding in platelets has

demonstrated the possible role of paxillin as a negative feedback regulator after integrin ligation to regulate the activity of Lyn tyrosine kinase [17]. However, this mode of regulation cannot fully explain the phenotypes of Pxn-KD platelets, because both outside-in and inside-out signaling were augmented by Pxn-KD. Our results reveal a new cellular function of paxillin and indicate new mechanisms that modulate platelet activation.

The most interesting result of this study was that Pxn-KD significantly enhanced the upstream signaling pathways that converge on platelet activation. Appropriate inhibition of the platelet response is essential to control pathological thrombus formation. It is well known that the mediators that enhance intracellular cAMP or cGMP



levels, including prostacyclin, prostaglandin E₁, and nitric oxide, are strong extrinsic inhibitors of platelet activation [27]. These extrinsic mediators ameliorate the broad platelet activation elicited by various agonists [27]. Intrinsic negative regulators of platelet activation have been identified recently, but many of these proteins only control a specific receptor signaling pathway. GPVI-mediated immunoreceptor tyrosine-based activation motif (ITAM) signaling is regulated by immunotyrosine-based inhibitory motif (ITIM)-containing receptors including platelet endothelial cell adhesion molecule 1 and carcinoembryonic antigen-related cell adhesion molecule 1 [28,29]. Furthermore, Lyn tyrosine kinase has been reported to inhibit ITAM signaling by inducing tyrosine phosphorylation of ITIM [28]. It has also been reported that binding of a regulator of G-protein signaling to the G₁₂ subunit limits platelet responsiveness to the receptor, which is independent of Rap1b [30]. Conversely, paxillin may downregulate platelet activity by modulating a common pathway,

because Pxn-KD resulted in marked platelet hyperactivation in response to stimulation of tyrosine phosphorylation-based receptors and G protein-coupled receptors.

Although paxillin is reportedly involved in various integrin-mediated cellular functions, many of these functions are limited to outside-in signaling pathways. Paxillin-deficient embryos show embryonic lethality, and the phenotype closely resembles that of fibronectin-deficient mice [31]. Moreover, paxillin-deficient fibroblasts show reductions in cell migration and tyrosine phosphorylation following cell adhesion [31]. Chimeric integrin αIIbβ3 with a cytoplasmic tail substitution of α4β1 or α9β1, which facilitates paxillin binding, significantly inhibits cell spreading, but does not affect αIIbβ3-dependent cell adhesion [18,19]. Inhibition of paxillin binding to integrin α4 inhibits leukocyte recruitment to an inflammatory site [32]. These data suggest important roles of paxillin in outside-in signaling by direct interaction with the integrin α-subunit. However, in this study, inside-out and outside-

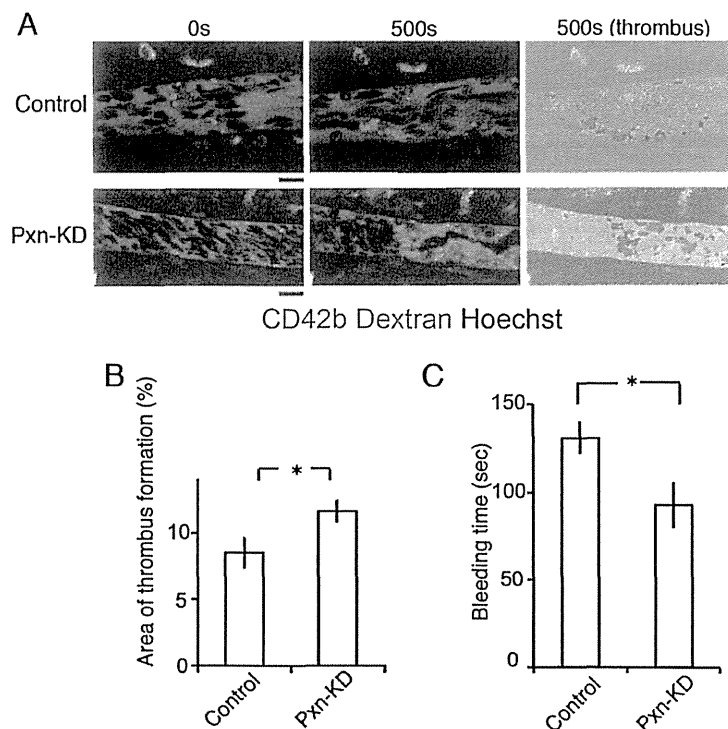


Figure 6 Pxn-KD in platelets expedites thrombus formation in vivo. (A) Intravital imaging of thrombus formation by laser irradiation of mesenteric arterioles in mice with control or Pxn-KD platelets. Thrombus formation was increased in mice with Pxn-KD platelets following laser irradiation. Bar, 10 μ m. The right panel shows the results of quantification of the thrombus area. (B) Percentage areas of thrombus within blood vessels after laser irradiation. Columns and error bars represent the mean \pm s.e.m. ($n = 40$ vessels in five mice/group). (C) Tail bleeding times were assessed as described in the Methods. Columns and error bars represent the mean \pm s.e.m. ($n =$ four mice/group). Statistical significance was determined using Student's *t*-test. * $P < 0.05$ vs. control.

in signaling of integrin α Ib β 3 were increased in Pxn-KD platelets, even though paxillin failed to interact with platelet-specific integrin α Ib [19]. It is possible that other signaling pathways in platelets are modulated by paxillin, which is independent of direct interactions with integrins.

An issue that remains unresolved is the precise mechanism governing the negative regulatory function of paxillin in platelet activation. As described above, Rathore et al. previously reported that integrin α Ib β 3-dependent platelet aggregation induced tyrosine phosphorylation of paxillin and Hic-5 in platelets, leading to the binding of Csk, which controls activation of the Src family of tyrosine kinases [17]. Csk preferentially binds to paxillin in murine platelets that coexpress paxillin and Hic-5 [17]. Furthermore, the interaction abolishes the activity of Lyn, but not Fyn or Src. It is possible that paxillin acts as a negative feedback regulator of outside-in signaling by modulating Lyn activity after ligand binding to integrin α Ib β 3 [17]. However, this mechanism does not fully explain the functional roles of paxillin in platelets. Our data suggest that paxillin controls additional proximal signaling pathways for platelet activation.

Pxn-KD did not directly augment the conformational changes of integrin α Ib β 3 expressed on Chinese hamster ovary cells (Additional file 9), tyrosine phosphorylation, or calcium mobilization induced by phosphoinositide turnover. These data suggest that paxillin negatively controls downstream signaling of calcium mobilization or a calcium-independent signaling pathway. In addition, calcium mobilization was rather reduced by Pxn-KD. It is therefore possible that negative feedback exists to prevent further activation of Pxn-KD platelets, or phosphoinositide turnover is directly modulated by Pxn-KD.

Our data suggest that several mechanisms may increase platelet activation by Pxn-KD. Notably, calcium-independent actions by Pxn-KD appear to exist, because P-selectin expression elicited by an agonist was still observed in Pxn-KD platelets even in the presence of BAPTA-AM. A previous report has suggested that coordinated signaling through both $G_{12/13}$ and G_i causes integrin α Ib β 3 activation, despite a small increase in intracellular calcium [33]. In addition, $G_{12/13}$ and G_i signaling activates integrin α Ib β 3 in G_q -deficient mice [34]. It is possible that paxillin modify the calcium-independent signaling

pathway leading to release reaction and integrin α IIB β 3 activation. Additional studies are needed to investigate how paxillin regulates platelet activation, and to assess whether these roles of paxillin in control of cellular signaling are common mechanisms in other cell types. We are now interested in further investigation of the precise mechanisms, and additional experiments are currently underway in our laboratory.

Another interesting finding of our study is that Pxn-KD resulted in an enlargement of platelet volume. CLP36, a member of the LIM domain family, was recently reported to play some roles in platelet activation [35]. Platelets from mice lacking the LIM domain of CLP36 show a slight increase in size and hyperactivation in response to a GPVI agonist [35]. The phenotypes of CLP36-deficient or mutant platelets are similar to those of Pxn-KD platelets in our study, although G protein-coupled receptor signaling is not affected in CLP36-deficient or mutant mice. Accordingly, the expression of LIM domain proteins may determine platelet size and reactivity.

To extrapolate the implications of our study to the biology and pathophysiology of humans, we must consider the differential expression pattern of paxillin-related proteins in platelets among species. Murine platelets express paxillin, Hic-5, and leupaxin, whereas human platelets only express Hic-5 [17]. Hagemann et al. reported that a switch from paxillin to Hic-5 expression should occur during the late phase of megakaryopoiesis in humans [15]. A recent report has described platelet functions in Hic-5-deficient mice [36]. Hic-5-deficient mice exhibit prolonged bleeding times, and the loss of Hic-5 in platelets slightly impairs integrin α IIB β 3 activation induced by thrombin, but not other agonists including convulxin, U46619, and ADP [36]. Although the hemostatic defect in Hic-5-deficient mice, as assessed by tail bleeding, is not fully explained by a mild defect in platelet function, it is possible that the structurally related proteins paxillin and Hic-5 play opposing roles in the regulation of platelet function in murine platelets. Leupaxin, another LIM protein that is predominantly expressed in leukocytes, has been reported to play an inhibitory role in B cell receptor signaling [37], which is similar to the role of paxillin reported in this study. In human platelets, which only express Hic-5, it will be necessary to elucidate whether Hic-5 acts as a positive regulator of integrin α IIB β 3 activation.

In summary, we have shown that paxillin is a negative regulator of platelet activation in mouse platelets. Modulation of platelet activation by Pxn-KD may originate in the augmentation of common signaling pathways, leading to integrin α IIB β 3 activation, release reactions, and Tx biosynthesis. Modulation of the LIM protein function might be an attractive candidate therapeutic target capable of strongly suppressing unexpected platelet activation in

thrombotic disorders. The next challenge will be elucidating the precise mechanism by which paxillin regulates the signaling pathway in platelet activation.

Additional files

Additional file 1: Schematic diagrams of the lentiviral vector used in this study. (A) Schematic diagram of the lentiviral vector. (B) Locations of the oligonucleotides encoding the shRNAs in the mouse *paxillin* (*Pxn*) gene. (C) Mouse embryonic fibroblasts were transduced with a lentiviral vector containing the control, Pxn-1, Pxn-2, or Pxn-3 shRNA sequences at MOIs of 1, 3, or 10. Protein expression was determined by immunoblotting at 48 h after transduction. Data are representative of three independent experiments.

Additional file 2: Oligonucleotide sequences of siRNA cloned into LentiLox.

Additional file 3: Pxn-KD does not affect granule contents. Bone marrow cells transduced with LentiLox-sh-control-GPIIb/IIIa (Control) or LentiLox-sh-paxillin-GPIIb/IIIa (Pxn-KD) at an MOI of 5 were transplanted into lethally irradiated recipient mice. (A) The morphology of control and Pxn-KD platelets was examined by transmission electron microscopy, and the areas of granules and cytoplasm in each platelet were independently quantified using ImageJ software for Macintosh. Columns and error bars represent the mean \pm s.d. ($n = 53-70$). (B-C) Washed platelets were lysed to measure the concentrations of platelet factor 4 (PF4) (B) and serotonin (C). Columns and error bars represent the mean \pm s.d. ($n = 4$). Statistical significance was determined using Student's *t* test. *** $P < 0.001$ vs. control.

Additional file 4: Expression levels of platelet-specific glycoproteins. Description of data: (A) Expression levels of GPIIb/IIIa (integrin α IIB β 3) (left panel), GPIb (middle panel), and GPVI (right panel) in control (dark gray) and paxillin-knockdown platelets (light gray). (B) Columns and error bars represent the mean \pm s.d. of the mean fluorescence intensity (MFI) of antibody binding ($n = 5$). Statistical significance was determined using Student's *t* test. * $P < 0.05$, ** $P < 0.01$, and *** $P < 0.001$ vs. control.

Additional file 5: Effects of apyrase and SQ29548 on agonist-induced integrin α IIB β 3 activation and P-selectin expression in control and Pxn-KD platelets. Platelets pretreated without or with 5 U/mL apyrase and 10 μ mol/L SQ29548 were stimulated with the indicated agonists. JON/A binding (A) and P-selectin expression (B) on GFP-positive platelets were assessed by flow cytometry. Column and error bars represent the mean \pm s.d. of the mean fluorescence intensity (MFI) ($n = 3-4$). Statistical significance was determined using Student's *t* test. * $P < 0.05$, ** $P < 0.01$, and *** $P < 0.001$ vs. control.

Additional file 6: Intravital imaging of thrombus formation by laser irradiation of mesenteric arterioles in mouse with control platelets.

Additional file 7: Intravital imaging of thrombus formation by laser irradiation of mesenteric arterioles in mice with Pxn-KD platelets.

Additional file 8: Thrombus formation in femoral arteries induced by FeCl₃. (A) Intravital imaging of thrombus formation 5 mins after FeCl₃ treatment in femoral arteries in mice with control or paxillin knock-down platelets (Pxn-KD). The black arrows indicate the direction of blood flow, and triangles show the developed thrombus. Bar, 100 μ m. (B) Areas of thrombus within arteries 20 mins after laser irradiation. Columns and error bars represent the mean \pm s.e.m. ($n = 8$ arteries in four mice/group).

Additional file 9: Knock-down of paxillin does not affect talin-dependent activation of integrin α IIB β 3 in CHO cells.

(A) Schematic representation of the lentiviral vectors used in this experiment. (B-D) α IIB β 3-CHO cells were transduced with lentiviral vectors expressing a control shRNA sequence and GFP (Control), the paxillin shRNA sequence and GFP (Pxn-KD), a control shRNA sequence and the GFP-Talin FERM domain (Control-FERM), or the paxillin shRNA sequence and the GFP-Talin FERM domain (Pxn-KD-FERM). (B) Lysates obtained from the transduced cells were immunoblotted with anti-GFP polyclonal antibody, anti-paxillin monoclonal antibody, and anti-vinculin monoclonal antibody. (C) PAC-1 binding after transduction in the presence or absence of 1 mmol/L GRGDS was assessed by